Geophysical Research Letters

Supporting Information for

How does El Niño Southern Oscillation Change Under Global Warming – A First Look at CMIP6

Hege-Beate Fredriksen[1]*, Judith Berner[2], Aneesh Subramanian[3], Antonietta Capotondi[4,5]

[1]Department of Physics and Technology, UiT the Arctic University of Norway, Tromsø, Norway.
[2]National Center for Atmospheric Research, Boulder, CO, USA.
[3]Atmospheric and Oceanic Sciences, University of Colorado Boulder, Boulder, CO, USA.
[4]Cooperative Institute for Research in Environmental Sciences, University of Colorado, Boulder, Colorado, USA.
[5]NOAA Physical Sciences Laboratory, Boulder, CO, USA.

Contents of this file

Introduction

This supporting information provides further details on the methods and analyses done in the main paper. Text S1 contains an extended description of the data and methods, Text S2 gives a brief discussion of the results of Figure S1, and Text S3 describes some background information for Figures S3 - S6.

Figure S1 shows spectra of the piControl Niño 3.4-index, Figure S2 shows the mean warming of in the Niño 3.4 region for future scenarios, Figures S3 and S4 show patterns associated with the E-index and C-index, Figure S5 shows the quadratic relationship of the two first principal components, Figure S6 the coefficient of the quadratic relationship plotted vs the skewness, and Figure S7 shows teleconnection patterns of sea level pressure for each model.

Text S1: Extended description of data and methods

Data

For the models BCC-CSM2-MR, CanESM5, MIROC6, MRI-ESM2-0, CESM2-WACCM we have used member r1i1p1f1 for all experiments. For models MIROC-ES2L, CNRM-CM6-1, MCM-UA-1-0, UKESM1-0-LL we have used member r1i1p1f2, except for MCM-UA-1-0 piControl, where r1i1p1f1 is used. For this model we note that historical r1i1p1f2 branches from piControl r1i1p1f1. For the model CNRM-ESM2-1 we have used member r1i1p1f2 for piControl, and its child member r2i1p1f2 for historical and future scenarios. For CESM2 we have used r1i1p1f1 for piControl and r4i1p1f1 for the other experiments.

For all piControl simulations, a linear trend is subtracted, to reduce a possible tiny influence of drift. For all future scenarios, a cubic spline detrending is used. When computing the trend, each of the future scenarios are first concatenated with the historical experiment. Then a cubic spline with two internal knots is fitted to the record from 1850 to 2100. The internal knots are chosen to be at the mid year (1932) and end year (2014) of the historical simulation. The only purpose of the historical data in this study is to improve the trend estimates of the future scenarios.

To ensure that the exact same region [5° S - 5° N, 170° W - 120° W] is used for all the models when computing the Niño 3.4-index, models' output is regridded to 1° x 1° degree resolution prior to spatial averaging. The data have monthly resolution, are smoothed by a 3-month running mean, and piControl mean seasonal variations are subtracted. The variances in Figure 2a and spectral analyses in Figure 1 are computed from anomalies obtained by detrending the Niño 3.4-index.

Spectral analysis

Spectral estimates are computed using Welch overlapped segment averaging on the Niño 3.4 index with monthly resolution. With this method we split the 86-yr long future scenarios into segments of 40 years, with 20 years overlap. For each segment, a windowed periodogram is computed with the Hanning window, then the results of each segment are averaged.

ENSO diversity

Following Cai et al. (2018), EOF analysis is applied to the region 15° S to 15° N, 140° E - 80° W. Before this analysis, models are regridded to a 1° x 1° grid to ensure the exact same regions are used for all models, then the monthly data are detrended and deseasonalized in each grid point. The first two EOFs and corresponding principal components are computed for piControl, then the two first principal components for future scenarios are estimated by projecting the data onto the piControl EOFs. All principal components are normalized by the estimated standard deviation of the first 500 years of piControl. As Cai et al. (2018) and Takahashi et al. (2011), we compute the E-index as (PC1 - PC2)/sqrt(2) and C-index as (PC1 + PC2)/sqrt(2), where the signs of the principal components are defined such that positive PC1 corresponds to positive anomalies in large parts of the Equatorial Pacific, and positive PC2 corresponds to positive anomalies in the western and negative in the eastern part of the Equatorial Pacific. Examples of E and C mode patterns are shown in Supplementary Figure 3.

ENSO teleconnections

An El Niño/La Niña event is defined to occur when the DJF mean exceeds +/- 1 standard deviation of the 3-month running mean piControl Niño 3.4-index from the same model. Preprocessing of the sea-level pressures are done as follows for each model: (i) DJF means are computed in all grid points, (ii) detrending in all grid points, (iii) find mean sea-level pressure for all DJF means classified as an El Niño or La Niña event, respectively. The model mean and standard deviations of these results are then computed in Figure 4, after regridding all models to a 1° x 1° grid.

Text S2: Power spectral density of piControl Niño 3.4-index

Supplementary Figure 1 shows that nine out of eleven models have a piControl spectral peak in the periodicity range 3-7 years. In the high-frequency end we find the model BCC-CSM2-MR, peaking at a period between 2 and 3 years, and in the low-frequency end we find MCM-UA-1-0, peaking at a period of 8 years.

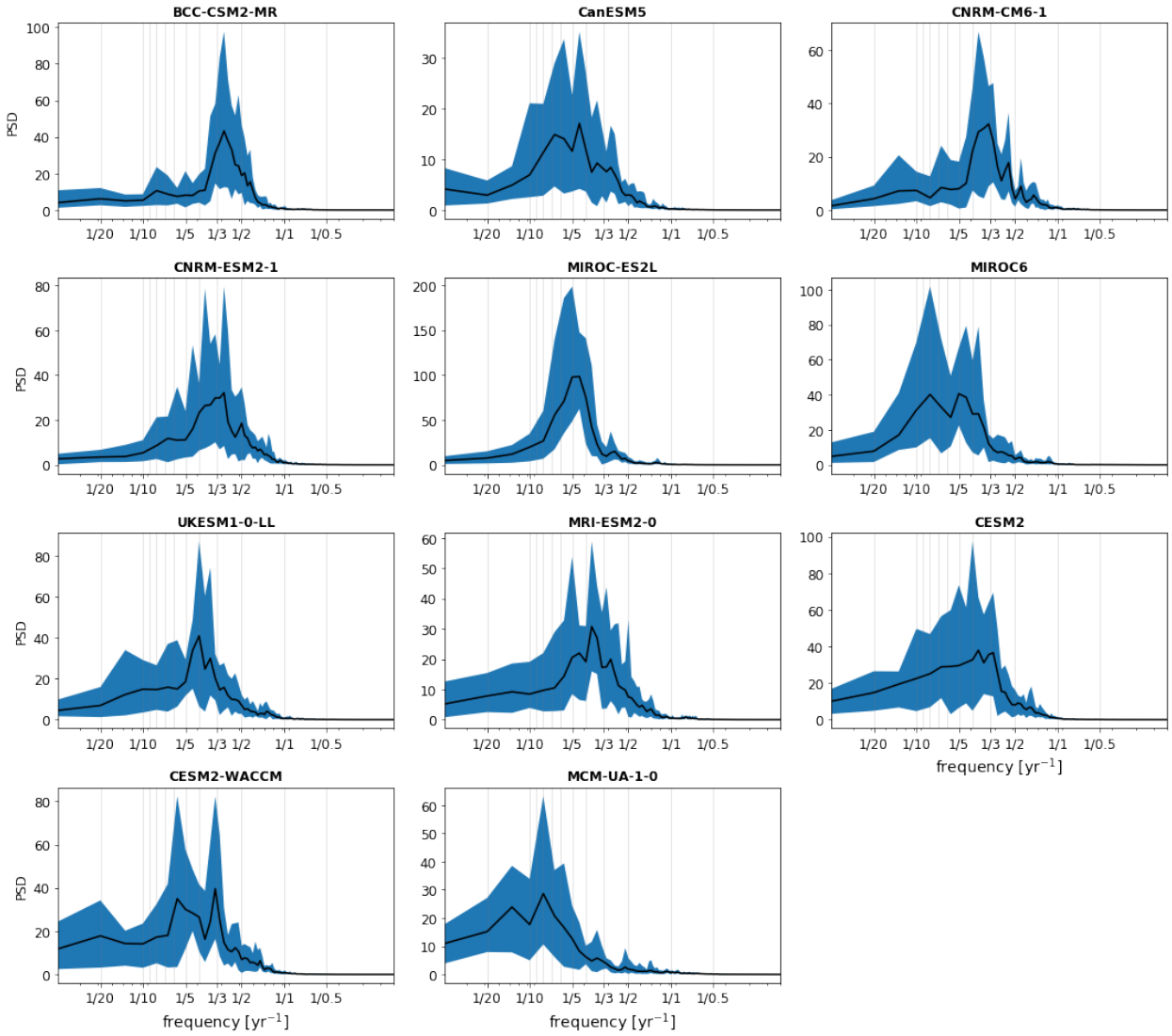

Figure S1. The black curves show the PSDs of the Niño 3.4-index computed using all of the first 500 years of piControl of each of the models. The shaded areas are the spread of the PSDs of 86-yr segments of the control runs, ranging from the minimum to the maximum values.

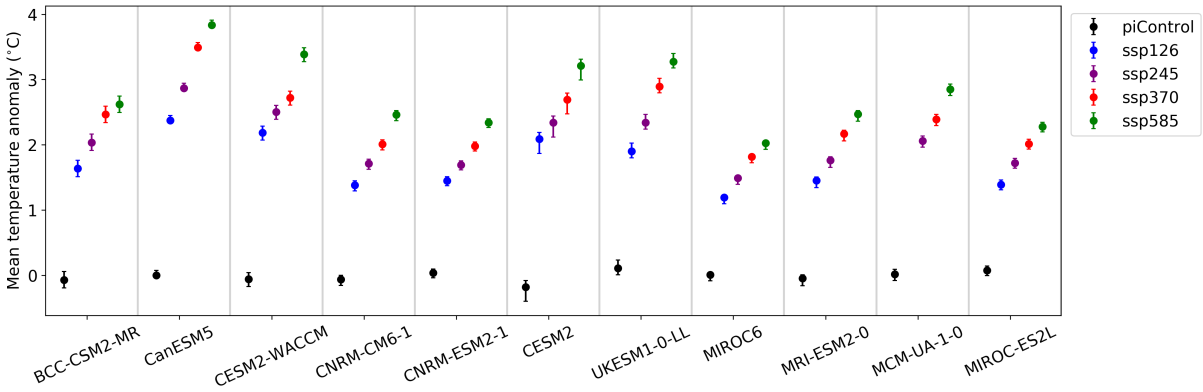

Figure S2: Mean temperature anomaly (°C) in the Niño 3.4 region [5° S - 5° N, 120° W - 170° W] for each of the CMIP6 models for piControl (black), and scenarios ssp126 (blue), ssp245 (purple), ssp370 (red) and ssp585 (green). The anomaly is computed as the difference between the time-averaged absolute temperatures from one member from each experiment and piControl, using monthly data with 3-month running mean. The error bars represent the spread of means in 86-year segments from piControl, ranging from the minimum to the maximum estimates.

Text S3: EP-ENSO and CP-ENSO patterns

The patterns associated with EP-ENSO and CP-ENSO are here calculated following the definition of Takahashi et al. (2011) as:

$$EP - ENSO\ pattern = \frac{\sqrt{2}}{2}(EOF1 \cdot std(PC1)\ -\ EOF2 \cdot std(PC2)) \quad (1)$$

$$CP - ENSO\ pattern\ = \frac{\sqrt{2}}{2}(EOF1 \cdot std(PC1)\ +\ EOF2 \cdot std(PC2)) \quad (2)$$

These expressions are derived such that:

$$PC1(t) \cdot EOF1 + PC2(t) \cdot EOF2 = C - index(t) \cdot CP - ENSO\ pattern\ +\ E - index(t) \cdot EP - ENSO\ pattern$$

The patterns obtained using this method are very similar to patterns obtained by performing a regression of the fields onto the C-index and E-index. The patterns for CESM2 are shown in Figure S3, and for the other models in Figure S4.

Following Karamperidou et al. (2017) and Cai et al. (2018), we estimate parameters in a quadratic relationship between PC1 and PC2:

$$PC2\ =\ \alpha\, PC1^2\ + \beta\, PC1\ +\ \gamma$$

The scatterplots of PC1-PC2, as well as the estimated values of α are shown in Figure S5, while the relationships between α and the skewness of the E and C indices (Cai et al., 2018) are displayed in Figure S6.

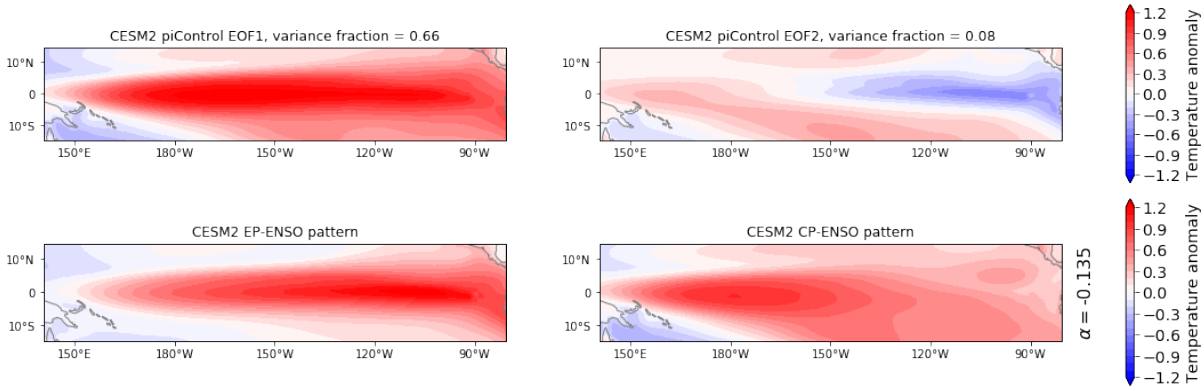

Figure S3: EOF1 and EOF2 for CESM2 (top row), and patterns associated with CP-ENSO and EP-ENSO (bottom row), calculated using Eqs. (1), (2). The patterns are scaled such that their corresponding principal component or index have standard deviation 1.

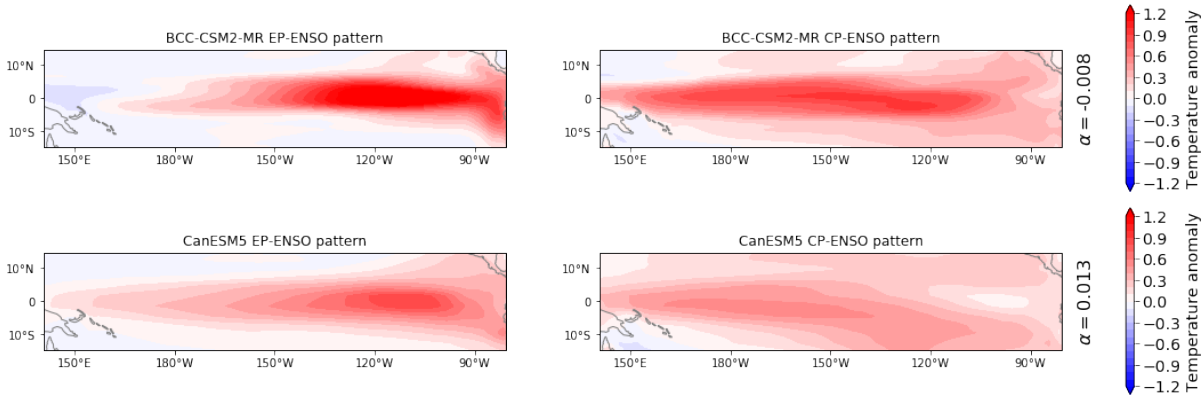

Figure S4: Patterns associated with CP-ENSO and EP-ENSO calculated using Eqs. (1), (2). The patterns are scaled such that their corresponding index have standard deviation 1.

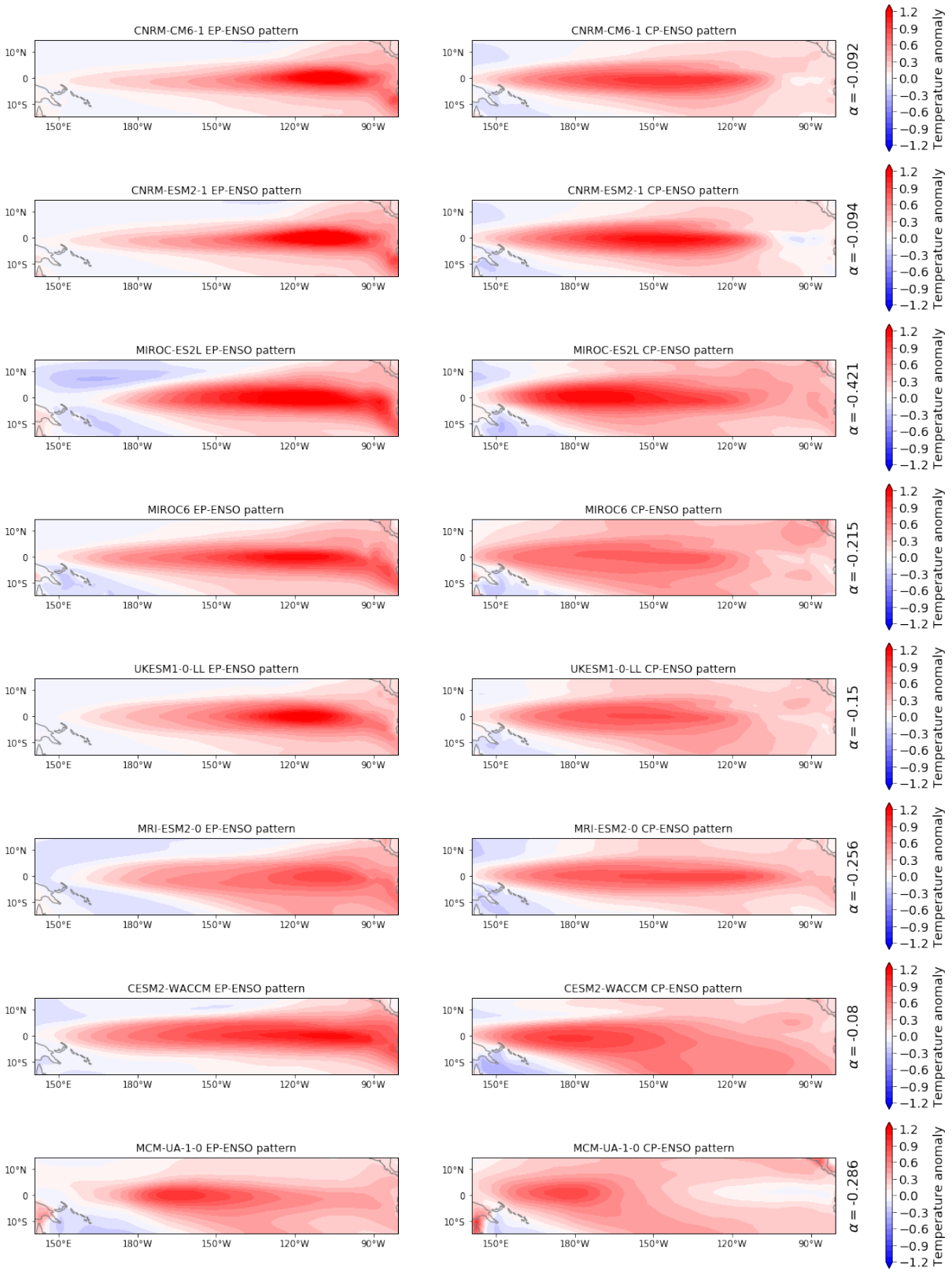

Figure S4 continued.

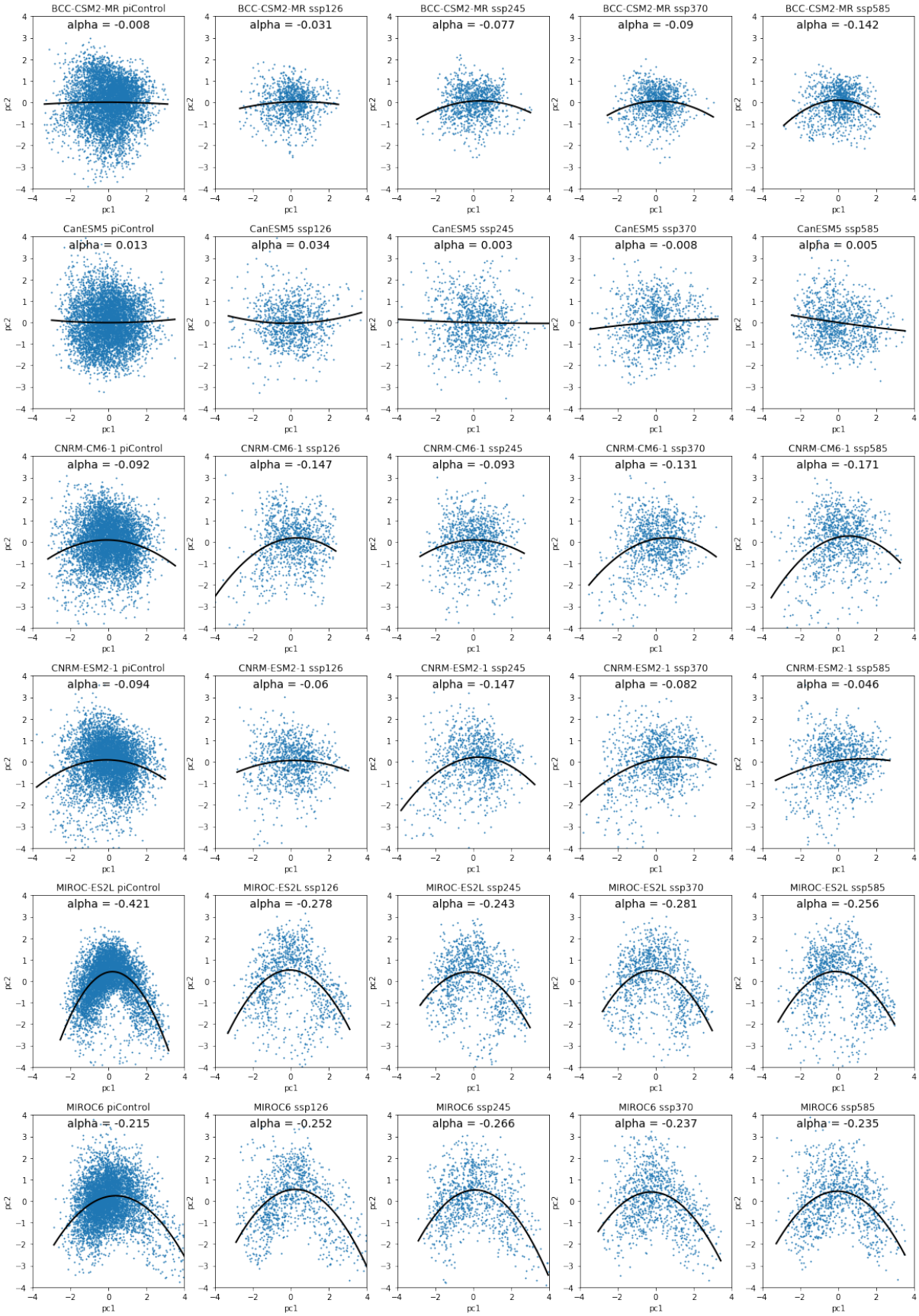

Figure S5: Scatterplots of PC1 vs PC2 for all models and scenarios in this study, and quadratic fits (black curves).

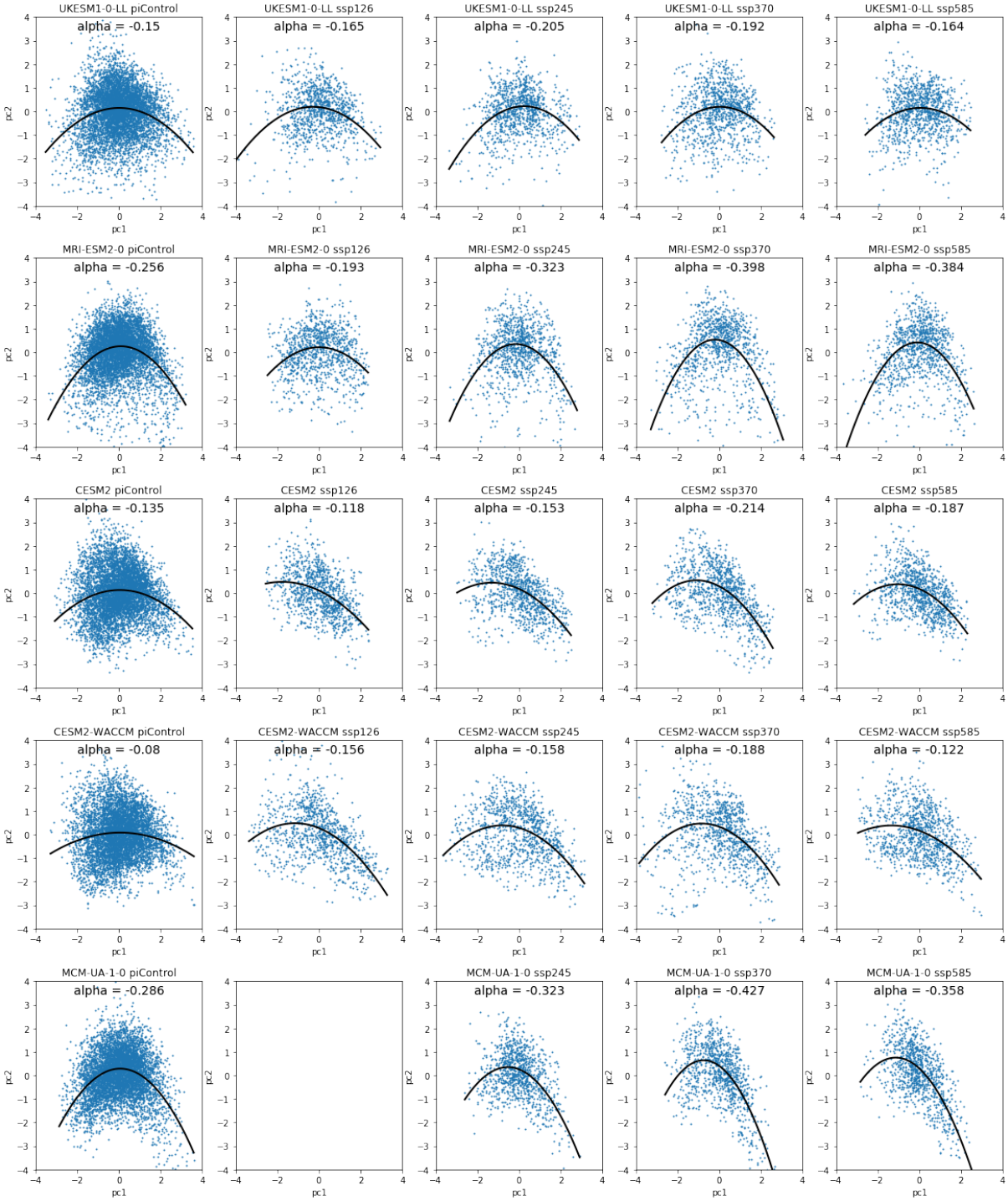

Figure S5 continued.

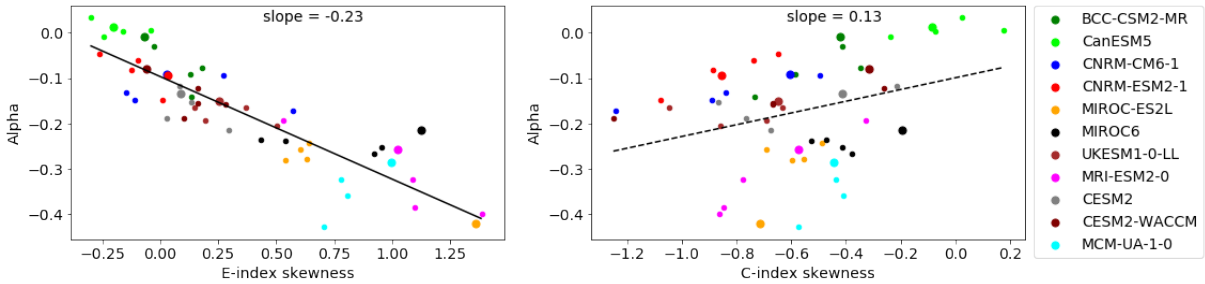

Figure S6: Estimates of alpha vs skewness of E-index and C-index. The five estimates for each model represent different experiments: large circles are from piControl, and used to sort models in main Figure 3, and the smaller circles are from SSP scenarios.

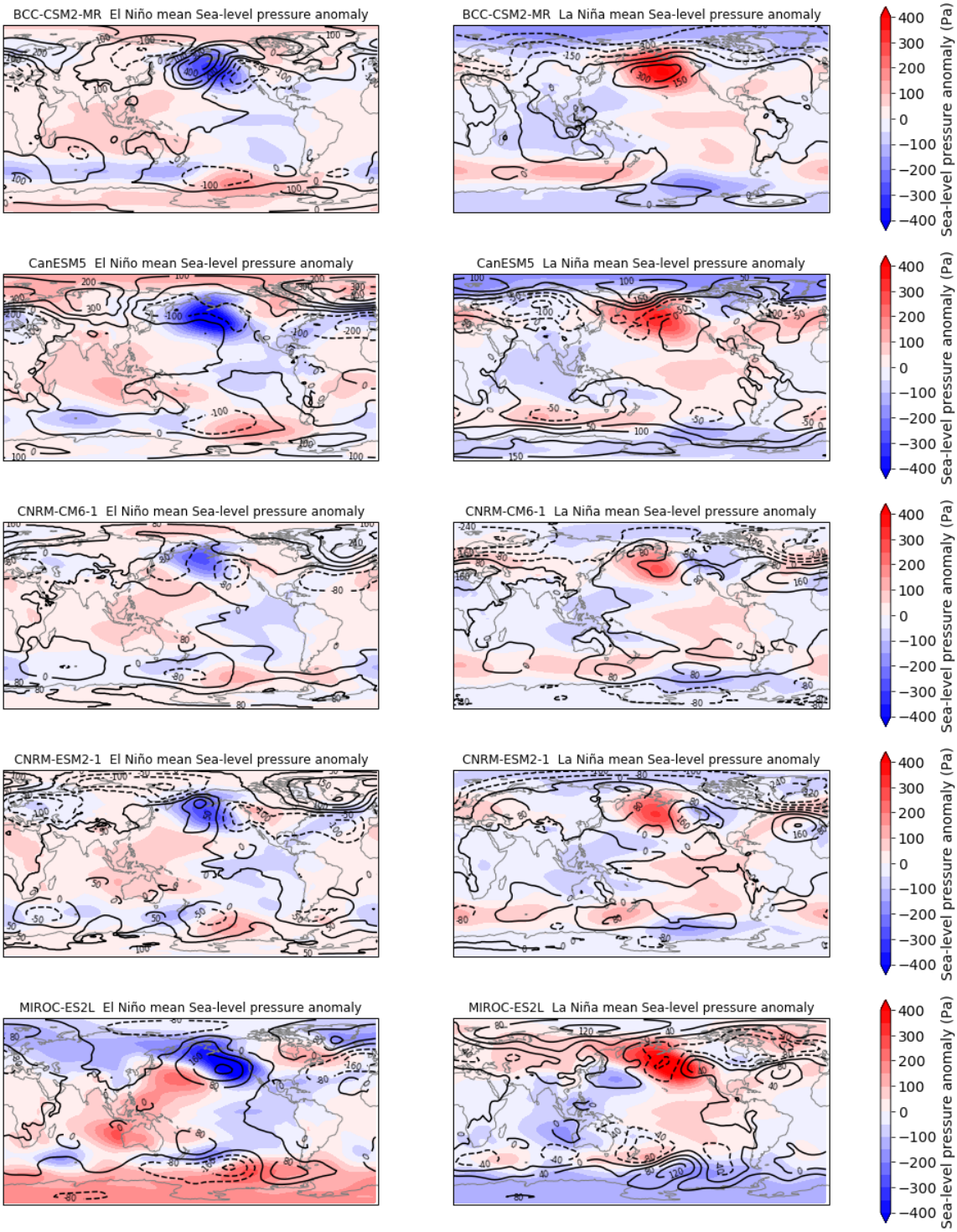

Figure S7: Showing the same as main Figure 4 a) and b), but for each model.

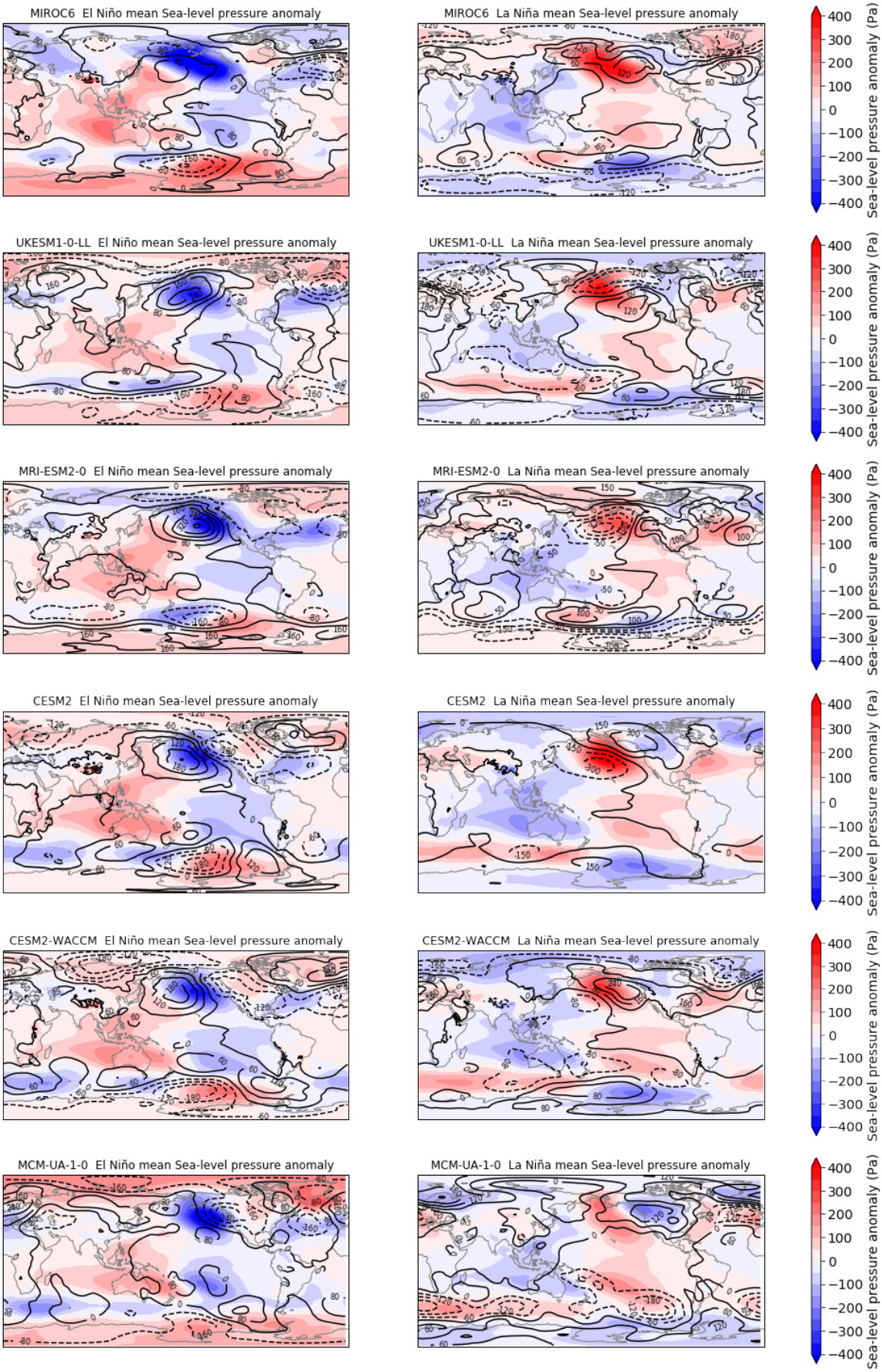

Figure S7 continued.